

Self-supervised Vector-Quantization in Visual SLAM using Deep Convolutional Autoencoders

Friday 15th July, 2022

Amir Zarringhalam^{1*}, Saeed Shiry Ghidary², Ali Mohades Khorasani³

¹Amirkabir University of Technology, Computer Science and Mathematics, 424 Hafez Ave, Tehran, Iran

²Staffordshire University, School of Digital, Technologies and Arts, College Rd, Stoke-on-Trent ST4 2DE, United Kingdom,
Amirkabir University of Technology, Computer Science and Mathematics, 424 Hafez Ave, Tehran, Iran

³Amirkabir University of Technology, Computer Science and Mathematics, 424 Hafez Ave, Tehran, Iran

Abstract: In this paper, we introduce AE-FABMAP, a new self-supervised bag of words-based SLAM method. We also present AE-ORB-SLAM, a modified version of the current state of the art BoW-based path planning algorithm. That is, we have used a deep convolutional autoencoder to find loop closures. In the context of bag of words visual SLAM, vector quantization (VQ) is considered as the most time-consuming part of the SLAM procedure, which is usually performed in the offline phase of the SLAM algorithm using unsupervised algorithms such as Kmeans++. We have addressed the loop closure detection part of the BoW-based SLAM methods in a self-supervised manner, by integrating an autoencoder for doing vector quantization. This approach can increase the accuracy of large-scale SLAM, where plenty of unlabeled data is available. The main advantage of using a self-supervised is that it can help reducing the amount of labeling. Furthermore, experiments show that autoencoders are far more efficient than semi-supervised methods like graph convolutional neural networks, in terms of speed and memory consumption. We integrated this method into the state of the art long range appearance based visual bag of word SLAM, FABMAP2, also in ORB-SLAM. Experiments demonstrate the superiority of this approach in indoor and outdoor datasets over regular FABMAP2 in all cases, and it achieves higher accuracy in loop closure detection and trajectory generation.

1. Introduction

Humans can benefit from autonomous vehicles and robots that operate long term in unaffordable circumstances, such as underground operations and navigating on the surface of other planets. Current autonomous navigation systems heavily depend on the Global Positioning System (GPS) for localization and navigation, which may not be available in many situations, such as populated urban areas, where skyscrapers stand and obscure the observable satellites. Also in indoor environments, GPS does not work reliably, since it depends on open sky factor.

Even when we are not limited by these factors, GPS does not provide us an accurate enough localiza-

*Correspondence: am.zarringhalam@aut.ac.com

tion. In such situations, robots can use visual SLAM for the purpose of navigation. In the last four decades, researchers have proposed many solutions to the terrestrial visual SLAM problem, which most of them use Kalman filters and sparse information filters to solve the SLAM problem. However, they can not produce large-scale maps, essentially due to the higher computational costs and uncertainties. For large-scale navigation, vSLAM plays a key role, however, there are mainly two issues happening while using the SLAM algorithm for large-scale scenarios. First, localization and positioning tend to drift for autonomous vehicles that are planing to drive over hundreds of kilometers in different air conditions. Second, maps do not necessarily remain viable under different driving conditions, and the positioning tends to deviate from the truth trajectory as the driving distance increases. Therefore, without prior knowledge of the environment, it is almost impossible to ensure correct localization of the vehicle over several kilometers. This results in turning our attention toward maps with sufficient localization accuracy. Several papers [1], [2] and [3] have addressed this problem by creating sub-map and multiple maps. However these methods impose proper data association assumption, to build large-scale maps that need consistent improvement. Therefore, these methods do not have a solution for large-scale implementation for increasingly unstructured environments. In this paper, we attempt to address the loop closure detection (LCD) problem, as the core of the vSLAM method, which is prone to many errors such as perceptual aliasing.

2. Related Works

Methods that have solved large scale loop closure detection using bag of words schema, up to now, are usually unsupervised, like SGNNS [4] which is the state of the art (in terms of speed) in this scope. Considering features extracted from sequence of images form a graph, SGNNS starts from a random node, while imposing a threshold on the nearest neighbor to that node, it incorporates KNN search and clusters the features. The main advantage of SGNNS over linear search and Kmeans, is its higher speed. Nevertheless, the constraint induced by this method for the nearest neighbor distance is inevitable. As another example Nishant, etal [5] proposed a bag of words pair (BoWP) based loop closure detection method that resolves the simple BoW method limitations like perceptual aliasing. This is achieved through incorporating the spatial occurrence of words in vector quantization procedure. They use a Bayesian probabilistic schema for loop closures detection.

As another example, iBoWLCD (incremental BoW loop closure detection) [6], proposes a novel appearance based model for loop closure detection. This method uses incremental BoW schema on binary features. It generates an on-line BoW without deleting any visual words learned during training.

In another work, Dorian Glovez [7] uses hierarchical BoW schema to detect revisited places. In order to build the hierarchical bag of words, which is structured as a tree, a set of binary features are first discretized to set of k cluster centroids, therefore a more compact representation of the features is obtained. The set of clusters constructed in this stage form the first level of the tree. This procedure is repeated on every cluster to make the subsequent levels of the tree.

To mention other examples, in [8] an appearance based method for loop closure detection, IBUILD (Incremental Bag of Binary Words for Appearance Based Loop Closure Detection), is presented. This approach focuses on building incremental binary vocabularies. This on-line method does not require learning vocabularies in every iteration of the SLAM algorithm, it only depends on scene appearance for loop closure detection. It also doesn't need GPS estimation and odometry information, because it builds vocabulary based on tracking the features between two consecutive images, to impose pose invariance assumption. Furthermore, this approach

uses simple likelihood function to generate suitable loop closure detection candidates. It also uses provisional consistency constraint to filter non-homogeneous closures out.

In another work [9], a method for pose graph optimization, and increasing performance of loop closure detection is presented. This is achieved using a combination of two novel metrics, expected information gain and visual word saliency. This paper uses global and local saliency to measure scarcity of an image in a dataset and en-richness of the candidate images for loop closure detection. The later measure is defined using bag of visual words histogram entropy for key-frames.

In PTAM (Parallel Tracking And Mapping) [10], that ORBSLAM is heavily based on, a camera pose detection method in an unknown scene is introduced. Although this issue has previously been well studied, PTAM introduces a parallelism, a method for tracking and mapping in small scale augmented reality framework. Specifically, tracking and mapping are attempted in parallel using two threads. One is in charge of tracking the cluttered hand movements, while other builds 3D map using extracted features from previously observed frames. This allows us to perform costly batch optimization operation in real time, which results in maps with thousands of land marks that can be tracked per frame with sufficient accuracy.

3. Methods

In this section, we briefly review the basic methods used in this paper. Our main modifications to these methods are also presented. First, we review the deep convolutional autoencoder (AE) used in this work. Next, we briefly review the FABMAP2 formulation, and introduce our novel method AE-FABMAP2 which integrates an AE for vector quantization. Then, we review ORB-SLAM and our modified version, AE-ORB-SLAM. We have also integrated an autoencoder on BoW SLAM which we explain at the end of this section.

3.1. Deep Convolutional Autoencoder (AE)

CAE is a model based on the encoder-decoder paradigm. First the encoder transforms the input into a lower dimensional space, then a decoder is regulated to reconstruct initial input from the low dimensional representation. This is achieved by minimizing of the cross entropy cost function [11]:

$$E = \frac{1}{N} \sum_{n=1}^N (y \log(\hat{y}_n) + (1 - y_n) \log(1 - \hat{y}_n)) \quad (1)$$

CAE uses convolution/deconvolution layers for the encoding/decoding part. These layers are followed by an activation function, and they are described as follows:

$$h^k = f\left(\sum_{l \in L} x^l \otimes w^k + b^k\right) \quad (2)$$

In Formula 2, k is the latent representation of the k^{th} feature map of the current layer, f is a non-linear activation function. \otimes denotes the 1D convolution operation, w^k and b^k are the weights (filters) and bias of the k -th feature map of the current layer, respectively. The CAE layers are arranged as follows:

Encoder:

- First layer consists of $32 - 3 \times 1$ filters followed by a max-pooling layer.
- The second layer will have $64 - 3 \times 1$ filters followed by a down-sampling layer.
- Final layer consists of $128 - 3 \times 1$ filters.

Decoder:

- First layer consists of $128 - 3 \times 1$ filters followed by a up-sampling layer.
- The second layer will have $64 - 3 \times 1$ filters followed by another up-sampling layer.
- Final layer consists of $1 - 3 \times 1$ filters.

3.2. Self-supervised Vector Quantization(SVQ)

Vector quantization is a sampling mechanism, which gets an input from elements of a vector space, and returns a set of indices denoted with i , as the result. The results are also coming from the same vector space. Here i refers to clustering centroids, which is a countable set, $i \in \{1, \dots, |\mathcal{C}|\}$, where $|\mathcal{C}|$ is the number of clustering that we get from applying a convolutional deep Autoencoder on the extracted SURF feature of the images. To be more specific, suppose D is the set of descriptors of a particular image in the database then:

$$Q(\hat{D})_i = \{j : \|D[i,] - C[j,]\|_2 \leq \|D[i,] - C[k,]\|_2 \forall k \in \{1, \dots, |\mathcal{C}|\}\} \quad (3)$$

is the quantized representation of features in that particular image.

3.3. FAB-MAP2

Here, we give a brief overview of the FAB-MAP2 algorithm. A detailed explanation of the algorithm can be found in[12]. FABMAP2 is a generative model which uses the following fact in the construction of BoW representation of images: Words that co-occur together usually originate from the same place. The configuration mentioned about FABMA2P, enables this method to detect places having too many features in common. In this method, the observation Z of an image at time k is reduced to some binary vectors. That is $Z_k = \{z_1, \dots, z_{|\mathcal{C}|}\}$, where z_i represents word i in the vocabulary, and indicates presence or absence of word i in the vocabulary. The vocabulary in FAB-MAP2 is obtained through clustering the extracted SURF features of the images using Kmeans. The overall observations up to time k is denoted by Z^k . The map of the environment is constructed from locations $\mathcal{L}^k = \{L_1, \dots, L_{n_k}\}$. Each of these locations is mapped to an appearance model, for example $L_i = \{p(e_i = 1|L_i), \dots, p(e_{|\mathcal{C}|} = 1|L_i)\}$. Suppose the robot is in the middle of the way and it has constructed a partial map of the environment. As the robot acquires new observation the likelihood of being in each of these locations is calculated, considering the observation up to the time i.e. $p(L_i|Z^k)$ is known. This term is obtained from the following formula:

$$P(L_i|Z^k) = \frac{p(Z_k|L_i, Z^{k-1})p(L_i|Z^{k-1})}{p(Z_k|Z^{k-1})} \quad (4)$$

In formula 4, $p(L_i|Z^{k-1})$ is the prior probability of the robot location, and $p(Z_k|L_i, Z^{k-1})$ is the observation likelihood.

To simplify the evaluation of $p(Z_k|L_i, \mathcal{Z}^{k-1})$, we suppose that observations in current time and the previous time are independent. Therefore using the naive Bayes formula we will have:

$$p(Z_k|L_i) \approx p(z_r|L_i) \prod_{q=1}^{|\mathcal{C}|} p(z_q|z_{P_q}, L_i) \quad (5)$$

In order to calculate the probabilities of absence of the observations in the map, it is needed to calculate $p(z^k|z^{k-1})$, to divide the map space into two parts: mapped and unmapped.

$$p(Z^k|Z^{k-1}) = \sum_{m \in \mathcal{L}^k} p(Z^k|L_m)p(L_m|Z_{k-1}) + \sum_{u \in \bar{\mathcal{L}}^k} p(Z^k|L_u)p(L_u|Z_{k-1}) \quad (6)$$

In formula 6, we can't compute the second term. Because it contains unvisited environments, though we can use mean field approximation to obtain this term, i.e: $p(Z_k|L_{avg}) = \sum_{u \in \bar{\mathcal{L}}^k} p(L_u|Z_{k-1})$, where $\sum_{u \in \bar{\mathcal{L}}^k} p(L_u|Z_{k-1})$ is the posterior probability of being a new place.

3.4. AE-FABMAP

In AE-FABMAP we have replaced the common unsupervised method Kmeans, with an autoencoder to quantize the image features. That is, after extracting the features from the image database, we feed them into a deep, 19 layer convolutional autoencoder to obtain the labels. Then, the cluster centroids and the BoW representation of the images are created using the obtained labels. Then, we fuse the BoW representation and cluster centroids obtained in the previous step into the FABMAP2 method to find the similarity between images in form of a confusion matrix. The general description of the method AE-FAMBAP is presented in Algorithm 1.

The general procedure of AE-FABMAP is described in algorithm 1. In this algorithm, part of LCD criteria is as follows: If the current observation matches a location with probability higher than a user specified threshold (e.g., $p > 0.999$), we associate the observation with that location [13].

A more detailed version of the algorithm 1 is described in the algorithm 2 and it's continuation in algorithm 3. In the first part of the algorithm 2, the default likelihood is calculated once (When a location is added to the map for the first time), that is we initialize the the locations default likelihood with d_1 . Here we assume a null observation with $z_q = 0$ for every q , and it is equal to the summation of D_q 's that is calculated for every word in the location. We also notice that the default likelihood is different for every location.

While processing new observation, the default likelihood of a place is adjusted using the variables d_2, d_3 and d_4 . In the next part of the algorithm 2 the observation likelihood are adjusted according to the content of current observation. That is, we consider the locations where q are observed in. All the log-likelihood of all locations are subtracted from the default value and they are updated with the proper values d_3 or d_4 . In the last part of the algorithm we consider the words, in which the observation occurs in the parent node of Chow-Liu tree but not the node itself, the log-likelihoods are adjusted with q_2 .

Algorithm 1. AE-FABMAP

Input: Training and Testing Images

Output: Confusion Matrix

```
1: procedure AE-FABMAP(Train Images, Test Images)
2:   Extract 128-d SURF features from all collected images
3:   Both for train and test dataset
4:   Apply PCA on the train and test images matrix
5:   Obtain BoW representation of train & test Datasets using an AutoEncoder
6:   Train a Chow-Liu tree (from training Dataset)
7:   i = Number of images in test dataset
8:   while i > 0 do
9:     Pick the row corresponding to the  $i^{th}$  image in the BoW representation
10:    Use a motion model calculate loop closure detection probability
11:    if LCD criteria is met then
12:      i - -
13:      Continue
14:    else
15:      Add new location
16:    end if
17:    i - -
18:  end while
19:  Return confusion matrix
20: end procedure
```

$$d2_{num} = \frac{CLtree(1, q) \times 0.61 \times (1 - CLtree(2, q))}{(1 - CLtree(1, q)) \times 0.39 \times CLtree(2, q)} \quad (7)$$

$$d_2 = \log\left(\frac{d2_{num}}{1 - d2_{den}}\right) - d_q \quad (8)$$

$$d2_{den} = \frac{CLtree(1, q) \times 0.61 \times CLtree(2, q)^2 \times 0.39}{[(1 - CLtree(1, q)) \times 0.61 \times (1 - CLtree(2, q)) + CLtree(1, q) \times 0.39 \times CLtree(2, q)] \times (1 - 0.39 \times CLtree(1, q))} \quad (9)$$

$$d3_{den} = \frac{0.61 \times CLtree(1, q) \times (1 - CLtree(1, q)) \times 0.39 \times CLtree(3, q)}{(1 - CLtree(1, q)) \times CLtree(1, q) \times 0.61 \times (1 - CLtree(3, q))} \quad (10)$$

$$d3_{num} = \frac{(1 - CLtree(1, q)) \times 0.39 \times CLtree(3, q)}{(1 - CLtree(1, q)) \times 0.39 \times CLtree(3, q) + CLtree(1, q) \times 0.61 \times (1 - CLtree(3, q))} \quad (11)$$

$$d_3 = \log\left(\frac{d3_{num}}{d3_{den}}\right) - d_q \quad (12)$$

$$d1^* = \frac{(1 - CLtree(1, q)) \times 0.61 \times (1 - CLtree(3, q))}{CLtree(1, q) \times 0.39 \times (1 - CLtree(3, q)) + (1 - CLtree(1, q)) \times 0.61 \times (1 - CLtree(3, q))} \quad (13)$$

Algorithm 2

```
1: Vector <Imatch> & matches
2: Vector test_Image_Descriptor
3: for  $i = 0$  ; # test _images ;  $i++$  do
4:   Vector <Imatch> QueryMatch
5:   Vector <Double> Default
6:   map <int, Vector <int> > inverted_map;
7:   for  $k = 0$  ; # test _images ;  $k++$  do
8:     Default.push_back(0);
9:     for  $q = 0$  ;  $q < CLtree(0,q)$  ;  $q++$  do
10:      if test_images(k)(0,q) > 0 then
11:        defaults.[end] += d1[q]
12:        inverted_map[q].append(defaults.size())
13:      end if
14:    end for
15:    Vector::iterator Lwidth, child;
16:    Vector<Double> likelihoods = Defaults;
17:    for  $q1 = 0$  ;  $q1 < CLtree.cols()$  ;  $q1++$  do
18:      if queryImgDescriptor(0,q1) > 0 then
19:        for Lwidth=inverted_map(q1).begin();Lwidth!=inverted_map(q1).end(); Lwidth++ do
20:          if queryImgDescriptor(0, $P_q(q1)$ ) > 0 then
21:            likelihoods[*Lwidth] +=  $d_4[q1]$ 
22:          else
23:            likelihoods[*Lwidth] +=  $d_3[q1]$ 
24:          end if
25:          for child=children(q1).begin();child!=children(q1).end(); child++ do
26:            if queryImgDescriptor(0,*child) == 0 then
27:              for Lwidth=inverted_map(*child).begin();
28: Lwidth!=inverted_map(*child).end(); Lwidth++ do
29:                likelihoods[*Lwidth] +=  $d_2[*child]$ ;
30:              end for
31:            end if
32:          end for
33:        end for
34:      end for
35:    end if
36:  end for
37: end for
38: for int k=0 ; likelihood.size() ;  $k++$  do
39:   QueryMatch.pushback(Imatch(0,k,likelihood(k),0));
40: end for
41: continued...
42: end for
```

Algorithm 3. Continued

```
1: for int j=1 ; QueryMatch.size() ;  $j++$  do
2:   QueryMatch[j].QueryIndx = i;
3: end for
4: matches.insert(matches.end(), QueryMatch.begin(), QueryMatch.end());
```

$$d_1 = \log(d1^*) \quad (14)$$

$$d4^* = \frac{CLtree(1, q) \times 0.61}{1 - 0.39 \times CLtree(1, q)} \quad (15)$$

$$d4 = \log(d4^*) - d_q \quad (16)$$

For each image, q is the index of the word in the vocabulary, and ranges from 0 to the $|\mathcal{C}|$. Filling confusion matrix can easily be achieved using the filled matches vector. d_3 and d_4 are used to calculate using log-likelihood based on the content current observation. d_2 is used to calculate log-likelihoods for unobserved words that are children of observed words in Chow-Liu tree. In [7 - 16], CLtree refers to Chow-Liu tree obtained from the BoW representaion of images and it is constructed using the deep CAE. For more information about Chow-Liu tree, see appendix B in [14]:

3.5. AE-ORB-SLAM

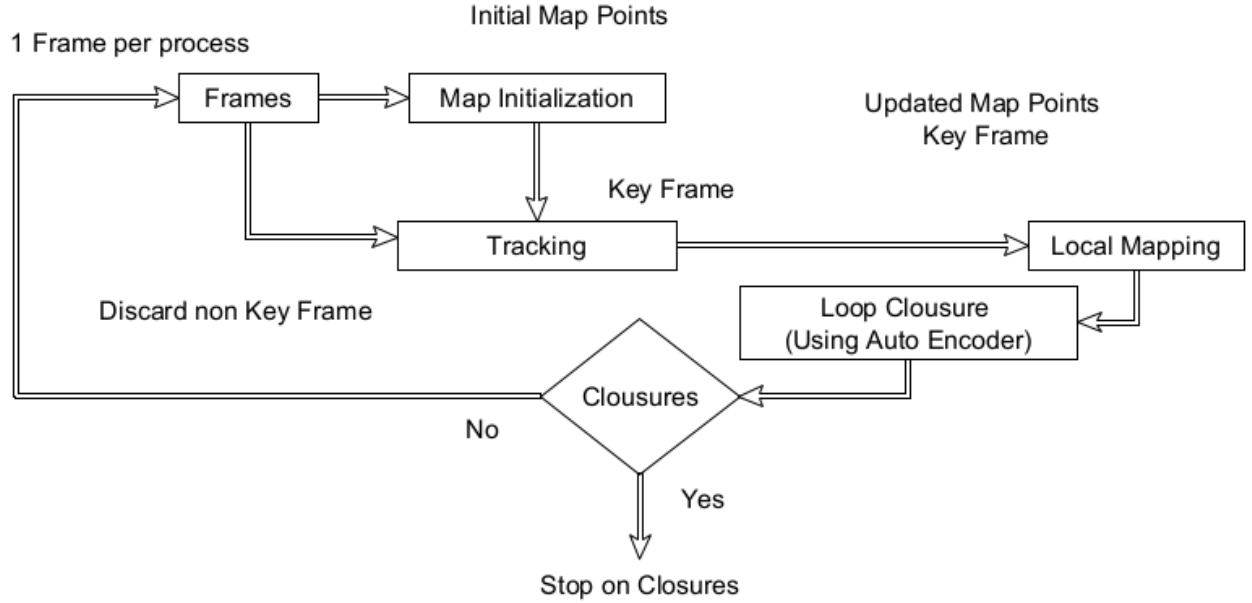


Figure 1: Pipeline of Deep Convolutional AE-ORB SLAM

As shown in pipeline of Figure 1, the AE-ORB SLAM procedure is roughly the same as ORB-SLAM [15], the only difference between these two SLAM algorithms is that in ORB-SLAM loop closure detection is computed by an unsupervised Kmeans clustering algorithm, while in AE-ORB-SLAM we replace that module with a self-supervised deep convolutional autoencoder. Furthermore, AE-ORB-SLAM starts with an initialization of the points in the map, in the 3D space. Next, 3D map points and relative camera position are computed using the extracted ORB features trough triangulation. In the tracking part, ORB-Features are matched with each

other. from first frame to the last, and the refined estimated camera pose is returned. In the local mapping, if an image is detected to be a key-frame, a 3D map point corresponding to that frame is placed in the 3D map, this is achieved using bundle adjustment. In the loop closure detection part, as mentioned before the BoW representation of images is constructed in the offline phase using a deep convolutional autoencoder.

3.6. AE-BoW

In regular BoW, the bag of words representation of images is obtained from cluster centroids. These centroids are the result of applying Kmeans to the standard image features. Furthermore, loop closure is detected by obtaining the cosine similarity of each image with all other images. In AE-BoW, we repeat the same procedure, except that instead of Kmeans, we embed a deep convolutional autoencoder to obtain the cluster centroids. This significantly increases the performance LCD.

4. Experimental Results

4.1. Metrics

In this article we have used the metrics used in [16]. It uses recall and accuracy of loop closure detection, They are defined as follows:

$$recall = \frac{\sum_i \sum_j ((Confusion\ Matrix[i][j] > threshold) \wedge ground\ truth[i][j] == 1)}{\sum_i \sum_j ground\ truth[i][j] == 1} \quad (17)$$

Each entry (i^{th}, j^{th}) of the ground truth matrix indicates whether images i and j were taken from the same location, if so, the entry is 1, otherwise it is zero. True Positives, the numerator of formula 17 and 18, is the number of elements in the confusion matrix greater than a given threshold, if their corresponding elements in the ground truth matrix are also ones.

Accuracy is defined as below:

$$accuracy = \frac{\sum_i \sum_j ((Confusion\ Matrix[i][j] > threshold) \wedge ground\ truth[i][j] == 1)}{\sum_i \sum_j (Confusion\ Matrix[i][j] == 1 > threshold)} \quad (18)$$

4.2. Datasets

The methods presented in this paper are tested on several indoor and outdoor datasets. The four methods BoW-SLAM, AE-Bow, FABMAP2 and AE-FABMAP are applied on Lip6 indoor dataset, TUM sequence 11, Stlucia (train/test), sequence 6 and 7 from Kitti dataset [17]. For ORB-SLAM the experiment is performed

on TUM Freiburg3 long office household. In the following section we briefly review the datasets used in this article. AE-FABMAP implementation is an extension to the the C++ package provided by [18].

4.2.1. Datasets used in AE-FABMAP and AE-BoW

Lip6indoor dataset*: Contains 387, 240 \times 192 images from a lab environment and contains several loops.

TUM sequence 11†: Contains 1500 images from a lab environment with different lighting condition. This dataset is collected from a narrow environment.

New College [Cummins and Newman 2008]: This dataset has been taken from the Oxford university campus which includes complex repetitive structures. This is an stereo dataset with left and right sequence. We have used the left sequence containing 1073 with resolution of 640 \times 480.

Newer College: Originally this dataset is a video (which we have converted into 200 image sequence). This dataset can be considered as a portion of new college dataset, it also has been collected at night and it contains 3 loops. In this dataset camera is experiencing cluttered movements.

Stlucia suburbs: There are two training and testing movies available for this dataset. Training data converted it to 540 images, and test dataset is converted to approximately 1000 images. This data set has been collected from saint Lucia suburbs. The environment in training and testing are roughly the same.

4.2.2. Dataset used in AE-ORB-SLAM

Freiburg3 ‡: This indoor dataset contains 2500 images taken from area around a table, and it contains one loop.

4.3. Results

Table 1 compares AE-FABMAP and FABMAP2 methods for the training datasets Saint Lucia(training), TUM sequence 11, Kitti sequence 6, New College and testing datasets Saint Lucia(testing), lip6indoor, Kitti sequence 7 and Newer College, respectively. The results are only reported for testing datasets in term of accuracy and recall. With the same datasets the experiment is repeated for algorithms AE-BoW and BoW, and the result of comparison is presented in Table 2. In these experiments, training and testing datasets are chosen in a way that they share a similar content but without any repeated path.

Next, we compare ORB-SLAM method with the newly introduced method AE-ORB-SLAM. Here we are outperforming ORB-SLAM algorithm, still the results are competitive. Absolute RMSE for key frame trajectory (m) for ORB-SLAM is 0.054353 and for our method it is 0.0473. To implement deep AE-ORB-SLAM we have modified the MATLAB ORB-SLAM package. §

*<https://animatlab.lip6.fr/AngeliVideosEn>

†<https://vision.in.tum.de/data/datasets/mono-dataset>

‡<https://vision.in.tum.de/rgbd/dataset/freiburg3/>

§<https://www.mathworks.com/help/vision/ug/monocular-visual-simultaneous-localization-and-mapping.html>

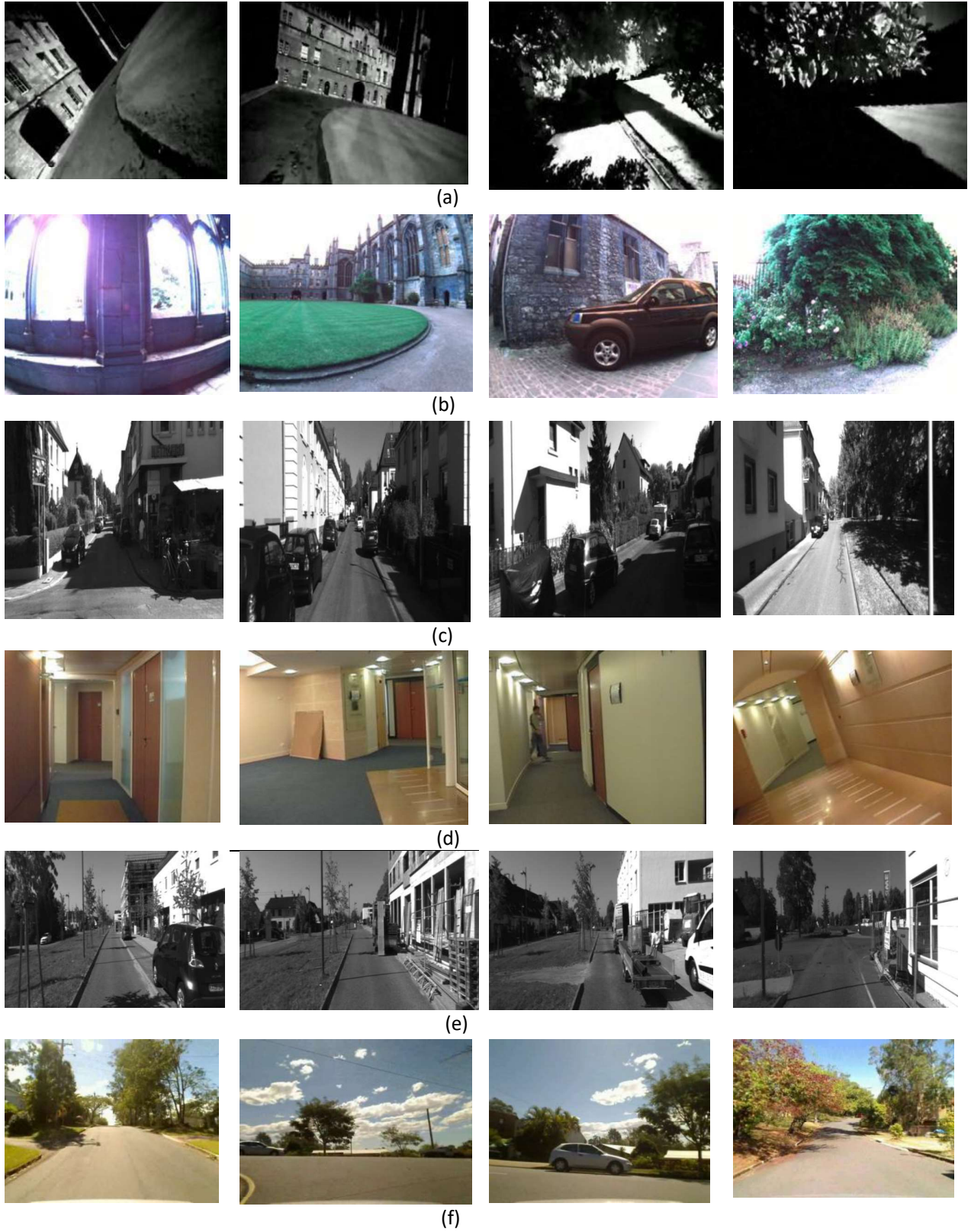


Figure 2: Datasets (a) Newer college, (b) New college, (c) Kitti sequence 7, (d) Lip6indoor, (e) Kitti sequence 6, (f) Stlucia (Tarin)

Table 1: Comparing AE-FABMAP and FABMAP2 methods for LCD.

Train Dataset	Test Dataset	AE-FABMAP		FABMAP2	
		%Acc	%Rec	%Acc	%Rec
Stlucia 311417	Stlucia 111417	% 74 % 83.5	% 79.12 % 69.5	%59.55	%81.5
TUM seq11 3924499	Lip6Indoor 27189	%60.8 % 59.55	%72.2 % 81.5	%52.59	%81.2
Kitti seq 6 227904	Kitti seq 7 235510	% 54.8 % 60 % 63.9	% 90.8 % 81.5 % 72.2	%51.1	%53
New College 160500	Newer College 194000	% 64.8 % 80.2	% 94.3 % 87.4	%60.1 %74.4	%89 %71.6

Table 2: Comparing AE-BoW and BoW methods for LCD.

Train Dataset	Test Dataset	AE-BoW		BoW	
		%Acc	%Rec	%Acc	%ReC
Stlucia 311417	Stlucia 111417	% 83.8	% 61.6	%83.6	%60
TUM seq11 3924499	Lip6Indoor 27189	% 82.4	% 82.1	%46	%80
Kitti seq 6 227904	Kitti seq 7 235510	% 60	% 75.6	%45	%71
New College 160500	Newer College 194000	% 71	% 87	%67	%87

The trajectory obtained from applying algorithms ORB-SLAM and AE-ORB-SLAM are shown in parts (a) and (c) of figure 3 respectively. In this figure ground truth is plotted in section (b).

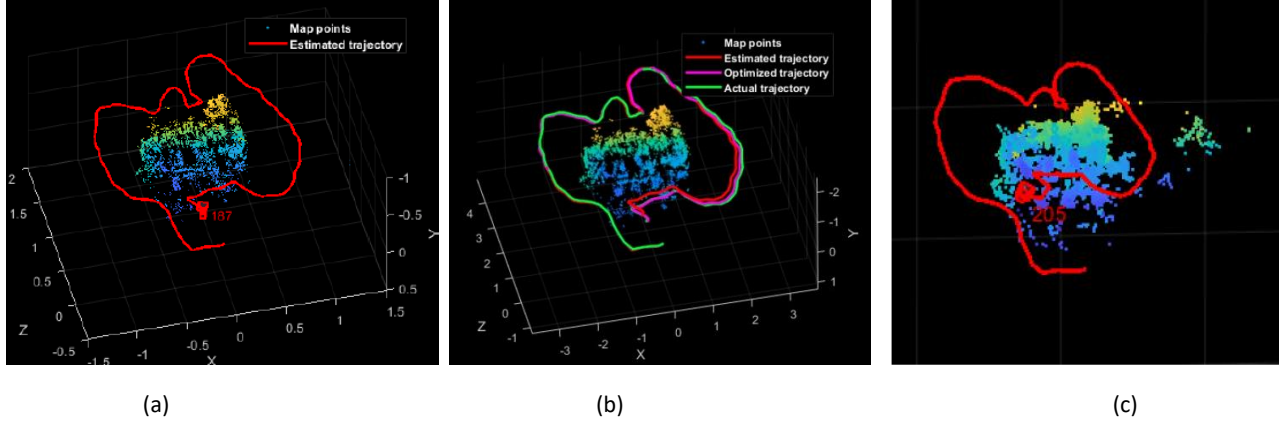


Figure 3: Trajectory of Freiburg3 dataset using (a) ORB-SLAM, (b) Ground truth and (c) AE-ORB-SLAM

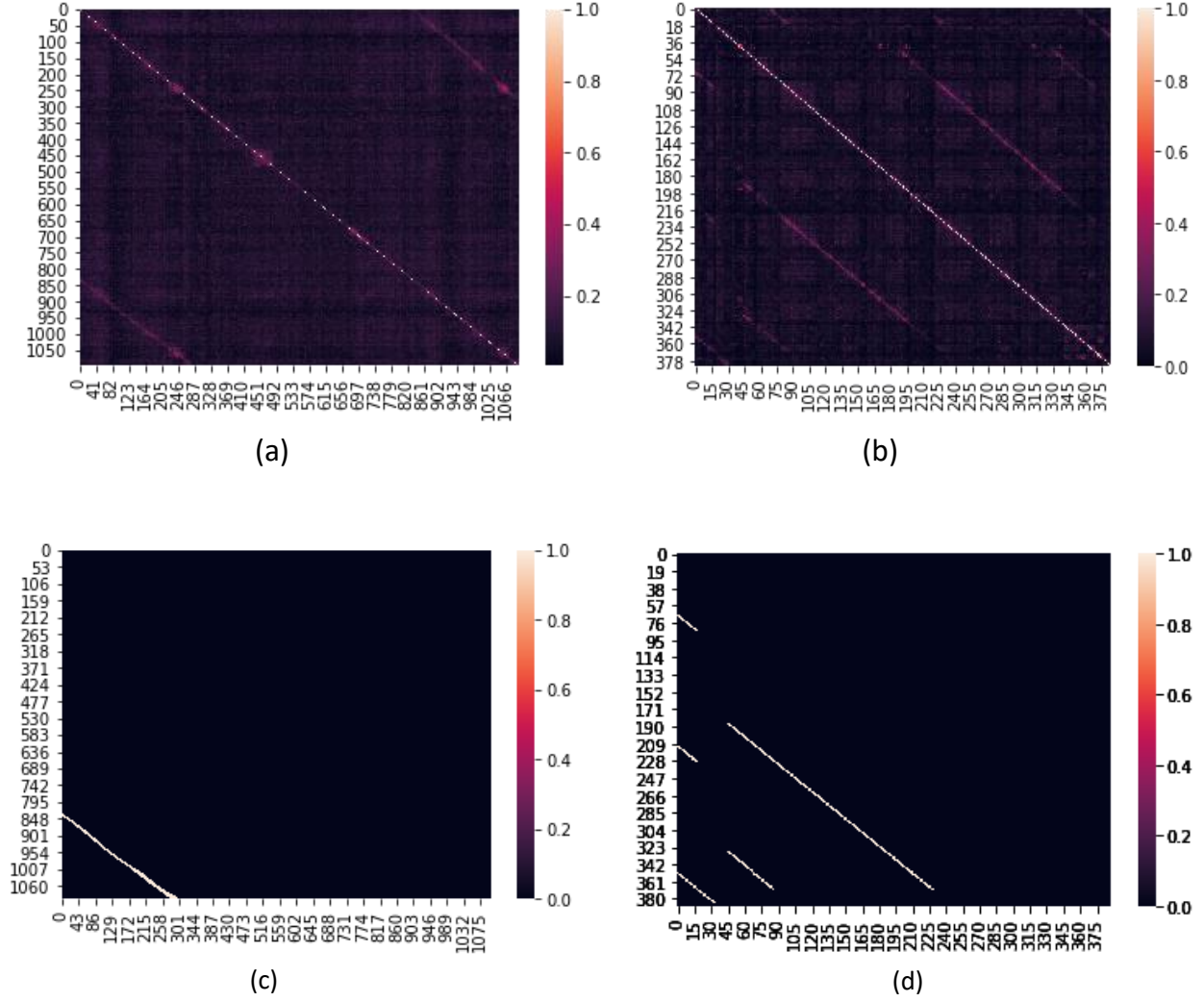


Figure 4: (a) Confusion matrix for Kitti dataset (sequence 6), (b) Confusion matrix for ip6indoor dataset, (c) Ground truth for Kitti dataset, and (d) Ground truth for ip6indoor dataset.

At the end of this section, for the sake of visual inspection of loop closures, we have plotted the result of AE-BoW (Due to it's fuzzy nature) applied on Lip6indoor dataset and Kitti sequence 6 dataset. These results are shown in figure 4 in terms of confusion matrices. The resulting confusion matrices are consistent with the datasets ground truths.

5. Conclusion

In this paper we introduced extensions to the current state of the art SLAM methods, and compared them with FABMAP2, ORB-SLAM and BoW. We concluded that the result of vector quantization module of the SLAM, may significantly enhance loop closure detection accuracy and recall. Our next task is to extend AE-FABMAP to operate on long range. This is achievable using deep autoencoders because as number of images

increases the number of features also grows, but the problem remains tractable using autocoders due to their efficiency in memory consumption. However we can apply autoencoders locally and join the clustering result using semi-supervised Latent Dirichlet Allocation, (LDA), to form the global clusters.

References

- [1] L. Paz, P. Jensfelt, J. Tardós, and J. Neira, “EKF slam updates in $O(n)$ with divide and conquer slam,” in *PROCEEDINGS OF THE 2007 IEEE INTERNATIONAL CONFERENCE ON ROBOTICS AND AUTOMATION, VOLS 1-10*, IEEE International Conference on Robotics and Automation ICRA, pp. 1657–1663, 2007. QC 20111221.
- [2] S. Se, D. G. Lowe, and J. Little, “Vision-based global localization and mapping for mobile robots,” *IEEE Transactions on Robotics*, vol. 21, pp. 364–375, 2005.
- [3] C. Estrada, J. Neira, and J. Tardos, “Hierarchical slam: real-time accurate mapping of large environments,” *IEEE Transactions on Robotics*, vol. 21, no. 4, pp. 588–596, 2005.
- [4] K. Hajebi and H. Zhang, “An efficient index for visual search in appearance-based SLAM,” *CoRR*, vol. abs/1309.7170, 2013.
- [5] N. Kejrival, S. Kumar, and T. Shibata, “High performance loop closure detection using bag of word pairs,” *Robotics and Autonomous Systems*, vol. 77, pp. 55–65, 2016.
- [6] E. Garcia-Fidalgo and A. Ortiz, “ibow-lcd: An appearance-based loop closure detection approach using incremental bags of binary words,” *CoRR*, vol. abs/1802.05909, 2018.
- [7] D. Gálvez-López and J. D. Tardós, “Bags of binary words for fast place recognition in image sequences,” *IEEE Transactions on Robotics*, vol. 28, pp. 1188–1197, 2012.
- [8] S. Khan and D. Wollherr, “Ibuild: Incremental bag of binary words for appearance based loop closure detection,” in *2015 IEEE International Conference on Robotics and Automation (ICRA)*, pp. 5441–5447, 2015.
- [9] A. Kim and R. M. Eustice, “Combined visually and geometrically informative link hypothesis for pose-graph visual slam using bag-of-words,” in *2011 IEEE/RSJ International Conference on Intelligent Robots and Systems*, pp. 1647–1654, 2011.
- [10] T. Pire, T. Fischer, G. Castro, P. D. Cristóforis, J. Civera, and J. J. Berles, “S-ptam: Stereo parallel tracking and mapping,” *Robotics and Autonomous Systems*, vol. 93, pp. 27–42, 2017.
- [11] V. Turchenko, E. Chalmers, and A. Luczak, “A deep convolutional auto-encoder with pooling - unpooling layers in caffe,” *CoRR*, vol. abs/1701.04949, 2017.
- [12] P. Newman, M. Chandran-Ramesh, D. Cole, M. Cummins, A. Harrison, I. Posner, and D. Schroeter, “Describing, navigating and recognising urban spaces - building an end-to-end SLAM system,” in *Proc. of the Int. Symposium of Robotics Research (ISRR)*, (Hiroshima, Japan), November 2007.
- [13] M. Cummins and P. Newman, “Accelerating fab-map with concentration inequalities,” *Robotics, IEEE Transactions on*, vol. 26, no. 6, pp. 1042–1050, 2010.
- [14] M. Cummins, *Probabilistic localization and mapping in appearance space*. PhD thesis, Oxford University, UK, 2009.
- [15] R. Mur-Artal, J. M. M. Montiel, and J. D. Tardós, “ORB-SLAM: a versatile and accurate monocular SLAM system,” *CoRR*, vol. abs/1502.00956, 2015.
- [16] Q. Zhong and X. Fang, “A bigbigan-based loop closure detection algorithm for indoor visual slam,” *Journal of Electrical and Computer Engineering*, vol. 2021, 2021.
- [17] A. Geiger, P. Lenz, and R. Urtasun, “Are we ready for autonomous driving? the kitti vision benchmark suite,” in *Conference on Computer Vision and Pattern Recognition (CVPR)*, 2012.

- [18] A. Glover, W. Maddern, M. Warren, S. Reid, M. Milford, and G. Wyeth, “Openfabmap: An open source toolbox for appearance-based loop closure detection,” in *The International Conference on Robotics and Automation*, (St Paul, Minnesota), IEEE, 2011.
- [19] A. J. Glover, W. P. Maddern, M. J. Milford, and G. F. Wyeth, “Fab-map + ratslam: Appearance-based slam for multiple times of day,” in *2010 IEEE International Conference on Robotics and Automation*, pp. 3507–3512, 2010.
- [20] T. N. Kipf and M. Welling, “Semi-supervised classification with graph convolutional networks,” *CoRR*, vol. abs/1609.02907, 2016.
- [21] I. Chami, Z. Ying, C. Ré, and J. Leskovec, “Hyperbolic graph convolutional neural networks,” in *Advances in Neural Information Processing Systems*, pp. 4869–4880, 2019.
- [22] I. Chami, R. Ying, C. Ré, and J. Leskovec, “Hyperbolic graph convolutional neural networks,” *CoRR*, vol. abs/1910.12933, 2019.
- [23] M. Cummins and P. Newman, “Appearance-only SLAM at large scale with FAB-MAP 2.0,” *The International Journal of Robotics Research*.
- [24] C. Mei, G. Sibley, M. Cummins, P. Newman, and I. Reid, “Rslam: A system for large-scale mapping in constant-time using stereo,” *International Journal of Computer Vision*, pp. 1–17, 2010. Special issue of BMVC.
- [25] B. Williams, M. Cummins, J. Neira, P. Newman, I. Reid, and J. Tardós, “A comparison of loop closing techniques in monocular slam,” *Robotics and Autonomous Systems*, 2009.
- [26] I. Posner, M. Cummins, and P. Newman, “A generative framework for fast urban labeling using spatial and temporal context,” *Autonomous Robots*, vol. 26, pp. 153–170, April 2009.
- [27] M. Cummins and P. Newman, “FAB-MAP: Probabilistic Localization and Mapping in the Space of Appearance,” *The International Journal of Robotics Research*, vol. 27, no. 6, pp. 647–665, 2008.
- [28] M. Cummins and P. Newman, “Invited Applications Paper FAB-MAP: Appearance-Based Place Recognition and Mapping using a Learned Visual Vocabulary Model,” in *27th Intl Conf. on Machine Learning (ICML2010)*, 2010.
- [29] C. Mei, G. Sibley, M. Cummins, P. Newman, and I. Reid, “A constant time efficient stereo slam system,” in *BMVC*, 2009.
- [30] M. Cummins and P. Newman, “Highly scalable appearance-only SLAM - FAB-MAP 2.0,” in *Proceedings of Robotics: Science and Systems*, (Seattle, USA), June 2009.
- [31] M. Cummins and P. Newman, “Accelerated appearance-only SLAM,” in *Proc. IEEE International Conference on Robotics and Automation (ICRA’08)*, (Pasadena, California), April 2008.
- [32] I. Posner, M. Cummins, and P. Newman, “Fast probabilistic labeling of city maps,” June 2008.
- [33] M. Cummins and P. Newman, “Probabilistic appearance based navigation and loop closing,” in *Proc. IEEE International Conference on Robotics and Automation (ICRA’07)*, (Rome), April 2007.
- [34] Sivic and Zisserman, “Video google: a text retrieval approach to object matching in videos,” in *Proceedings Ninth IEEE International Conference on Computer Vision*, pp. 1470–1477 vol.2, 2003.
- [35] B. Williams, M. Cummins, J. Neira, P. Newman, I. Reid, and J. Tardos, “An image-to-map loop closing method for monocular SLAM,” in *Proc. International Conference on Intelligent Robots and Systems*, 2008.
- [36] J. Aulinas, Y. Petillot, J. Salvi, and X. L. A, “The slam problem: a survey,” 2008.
- [37] K. Hajebi, Y. Abbasi-Yadkori, H. Shahbazi, and H. Zhang, “Fast approximate nearest-neighbor search with k-nearest neighbor graph,” in *IJCAI*, 2011.
- [38] J. Sturm, N. Engelhard, F. Endres, W. Burgard, and D. Cremers, “A benchmark for the evaluation of rgb-d slam systems,” *2012 IEEE/RSJ International Conference on Intelligent Robots and Systems*, pp. 573–580, 2012.
- [39] R. E. González Valenzuela, W. R. Schwartz, and H. Pedrini, “Dimensionality reduction through pca over sift and surf descriptors,” in *2012 IEEE 11th International Conference on Cybernetic Intelligent Systems (CIS)*, pp. 58–63, 2012.

- [40] G. Klein and D. Murray, “Parallel tracking and mapping for small ar workspaces,” in *2007 6th IEEE and ACM International Symposium on Mixed and Augmented Reality*, pp. 225–234, 2007.
- [41] J. Johnson, M. Douze, and H. Jégou, “Billion-scale similarity search with gpus,” *arXiv preprint arXiv:1702.08734*, 2017.